Check for updates

Optical discrimination of histamine and ethylenediamine in meat samples using a colorimetric affordable test strip (CATS): introducing a novel lab-on paper sensing strategy for low-cost ensuring food safety by rapid and accurate monitoring of biogenic amines†

Arezoo Saadati,[a] Fatemeh Farshchi,[b] Mohsen Jafari,[c] Houman Kholafazad, [iD][d] Mohammad Hasanzadeh [iD] *[e] and Nasrin Shadjou [iD][f]

Biogenic amines (BAs) are a group of organic compounds that are produced through the decarboxylation of amino acids by microorganisms. These compounds are commonly found in a variety of foods and are known to cause adverse health effects if consumed in high concentrations. Therefore, the development of sensitive and rapid detection methods for detection and determination of BAs is essential for ensuring food safety. In this study, a novel colorimetric affordable test strip (CATS) was developed for the colorimetric and naked-eye detection of two BAs of ethylenediamine (EDA) and histamine (HIS) in meat samples. Also, triangular silver nanoparticles (AgNPrs) were used as a diagnostic optical probe, and CATS used as a simple, environmentally friendly, inexpensive diagnostic substrate for on-site recognition of meat spoil. The AgNPrs-based optosensor demonstrated high sensitivity and selectivity towards EDA and HIS, allowing for the detection of low concentrations of the BAs in real food samples such as raw chicken and beef. The system presented a UV-vis technique for HIS and EDA analysis in the linear range of 0.1 μM to 0.01 mM, with an LLOQ of 0.1 μM, and 0.05 to 1 μM, with an LLOQ of 0.05 μM, respectively. Additionally, the performance of the designed CATS in the analysis of produced gases was evaluated, highlighting the potential of this simple and cost-effective strategy for the development of BAs diagnostic kits. This approach provides a simple and cost-effective method for detecting BAs in food, which could be beneficial for ensuring food safety and preventing the harmful effects associated with their consumption.

1. Introduction

Biogenic amines (BAs) are small organic molecules with a hydroxyl, aromatic, and aliphatic structural base, which show high biological activity.[1,2] They are mainly created in the tissues of living organisms because of enzymatic decarboxylation of

[a]*Nutrition Research Center, Tabriz University of Medical Sciences, Tabriz, Iran*
[b]*Fundação Oswaldo Cruz, Instituto Oswaldo Cruz, Laboratório de Biologia Molecular e Doenças Endêmicas, Avenida Brasil No 4365-Manguinhos, Rio de Janeiro 21040-900, RJ, Brazil*
[c]*Biotechnology Research Center, Tabriz University of Medical Sciences, Tabriz, Iran*
[d]*Food and Drug Safety Research Center, Tabriz University of Medical Sciences, Tabriz, Iran*
[e]*Pharmaceutical Analysis Research Center, Tabriz University of Medical Sciences, Tabriz, Iran. E-mail: hasanzadehm@tbzmed.ac.ir*
[f]*Department of Nanotechnology, Faculty of Chemistry, Urmia University, Urmia, Iran*
† Electronic supplementary information (ESI) available. See DOI: https://doi.org/10.1039/d4ra00101j

amino acids and transamination of aldehydes and ketones.[3] BAs are present in fresh food, particularly in protein-rich samples, and their levels may rise due to improper storage. While BAs can serve as hormones and neurotransmitters, excessive amounts can result in toxicity.[4]

Histamine (HIS) is one of the most bioactive and toxic BAs that can cause an allergic reaction in humans. According to the European Food Safety Authority, the US Food and Drug Administration, and the World Health Organization, there are ranges of BAs concentrations in food that indicate food quality.[5] For example, a concentration of fewer than 50 mg kg^{-1} of HIS indicates good quality fresh food. A concentration between 50 and 200 mg kg^{-1} leads to toxic effects on humans, and a concentration above 200 mg kg^{-1} causes poisoning in humans. The allowed concentration of other BAs is higher than HIS.[6] Therefore, as a result, the surveillance of BAs as a key metric holds significant value in the analysis and management of food quality.

Improper storage of meat can lead to the formation of BAs, which are created through microbial enzymatic processes such as the conversion of amino acids *via* decarboxylation and the transformation of organic compounds containing carbonyl groups.[7] The accumulation of BAs can indicate that food has spoiled. Most BAs have a bad smell, are poisonous, and carcinogenic, causing headaches, heart palpitations, mucosal burns, eye, and respiratory system irritation.[8]

Detection of BAs in food is very challenging due to their high polarity and higher solubility in water compared to organic solvents.[9] Various methods such as high-performance liquid chromatography,[10] gas chromatography,[11] capillary electrophoresis,[12] mass spectrometry[13] and enzyme-linked immunosorbent assay (ELISA)[1] have been developed for the determination of BAs in food. The methods described, while displaying high sensitivity and selectivity, call for technicians who have received specialized training and developed skills.[14] The current detection methods for amines are associated with several limitations, including complicated sample preparation, high instrumentation expenses, the need for trained professionals, susceptibility to environmental interferences, expensive reagents, and time-consuming sample preparation.[15] As a result, they are rarely utilized for on-site amine detection. With increased demands for monitoring toxic substances in food, it is difficult to create sensors capable of detecting amines at ppb levels.[16]

Colorimetric sensor arrays are a good option due to their environmental tolerance, high selectivity, and ability to recognize numerous analytes.[17] They have several advantages, such as simple sampling methods, visual sensing mechanism, and easy miniaturization, making them ideal for amine detection with results obtainable within minutes.[18] Colorimetric techniques have gained special importance due to their easy operation, ease of use, high sensitivity, and high selectivity that can be detected by the naked-eye.[19]

On the other hand, UV-visible spectroscopy can be used as a cheap and simple analytical method to study BAs.[20] The combination of optical sensing systems with miniaturized microfluidic paper-based devices like colorimetric affordable test strip (CATS) can provide an opportunity for early screening of food samples by home users and food industries in food chains worldwide.[21] A colorimetric affordable test strip is a low-cost diagnostic tool that uses color changes to detect the presence of specific substances in a sample. These test strips are typically made of paper or plastic and are impregnated with chemical reagents that react with the target analyte to produce a visible color change. The color change can then be compared to a color chart to determine the concentration of the analyte in the sample.[22] Colorimetric affordable test strips are widely used in a variety of applications, including: (I) medical diagnostics: colorimetric test strips are used to detect a wide range of medical conditions, including diabetes, pregnancy, and urinary tract infections.[23] (II) Environmental monitoring: colorimetric test strips are used to detect pollutants in water, soil, and air.[24] (III) Food safety: colorimetric test strips are used to detect foodborne pathogens and toxins.[25] (IV) Industrial quality control: Colorimetric test strips are used to monitor the quality of raw materials and finished products.[26] Their simplicity is due to the creation of hydrophilic microchannels on cellulose using a variety of hydrophobic materials such as wax, paraffin, polymers, and ink. So, colorimetric affordable test strips are a simple, inexpensive, and user-friendly way to detect the presence of specific substances in a sample. They are widely used in a variety of applications and can provide valuable information for medical diagnosis, environmental monitoring, food safety, and industrial quality control.

In recent years, nanomaterial such as carbon nanotubes, graphene, and metal nanoparticles have significantly utilized to improvement of the speed and cost of analysis. As a result, the nanoparticles change color upon interaction with the analyte and help in visual detection. Metal nanoparticles have attracted the attention of many researchers due to their high surface plasmon resonance. Compared to gold nanoparticles (AuNPs), silver nanoparticles (AgNPs) have plasmon resonance with lower wavelengths and higher intensity. In addition, the peaks in AgNPrs are sharper and stronger and show more sensitivity to the refractive index of the surrounding environment.[27] Silver nanoprisms (AgNPs) exhibit distinct optical, electrical, and chemical characteristics in contrast to spherical AgNPs.[28] Also, AgNPs have strong properties of surface plasmon resonance according to the shape, which can be adjusted by changing the thickness, edge length and morphology of the tip of the nanoplate.[29–31]

The current study introduces a novel and highly sensitive colorimetric tool for the detection of HIS and ethylenediamine (EDA) in raw beef, utilizing triangular silver nano-prism (AgNPrs) as diagnostic probes. The technique depends on detecting the alteration in color and absorption spectrum caused by the interplay of the sensing probes with the ions generated from the gases, showcasing the method's capability to specifically detect the target amines. Furthermore, the efficacy of the developed affordable colorimetric test strip (CATS) in analyzing the produced gases was assessed, underscoring the promise of this uncomplicated and economical approach for creating diagnostic kits for BAs.

2. Experimental

2.1. Chemicals and materials

EG (ethylene glycol), silver chloride (AgCl), polyvinyl pyrrolidone (PVP K-30), H_2O_2 (hydrogen peroxide), $C_6H_{15}N$ (triethylamine), $NaBH_4$ (sodium borohydride), NaOH (sodium hydroxide), CH_3COOH (acetic acid), KI (potassium iodide), $AgNO_3$ (silver nitrate), $Na_3C_6H_5O_7$ (tri-sodium citrate), HIS and EDA were bought from Sigma-Aldrich (Ontario, Canada). This study was ethically approved by Tabriz University of Medical Science (TBZMED), Tabriz, Iran (IR.TBZMED.VCR.REC.1401.145).

2.2. Instruments

UV-vis spectroscopy was analyzed using the U-3010 spectrophotometer from Hitachi, Japan. The particle size and shape of the nanoparticles were examined using transmission electron microscopy (TEM) with an operating voltage of 200 kV from Adelaide, Australia. Atomic force microscopy (AFM) with

Nanosurf (AG Gräubernstrasse 124, 410 Liestal Switzerland) in tapping mode was employed to investigate the dynamic size of nanoparticles. For surface morphology assessment of synthesized nanoparticles, high-resolution field-emission scanning electron microscopy (FE-SEM, Hitachi-Su8020, Czech-with a working voltage of 3 kV) was used. The elemental composition of nanoparticles was evaluated using energy-dispersive spectroscopy (EDS). Zeta potential measurement and dynamic light scattering (DLS) analysis were used to determine the surface charge and size distribution using Zetasizer Ver.7.11 and Malvern Instruments Ltd, MAL1032660, England.

2.3. Synthesis of AgNPrs

Nanoparticle synthesis was performed according to our previous work with brief modification.[30] In the initial step of AgNPrs synthesis, 0.06 g of PVP was dissolved in 3 mL of deionized water (DW) and subsequently added to 200 mL of DW. In the subsequent step, 4 mL of $AgNO_3$ (0.01 M) were added and agitated for a duration of 3 minutes, following which 8 mL of TSC (75 mM) and 960 μL of H_2O_2 were added and stirred vigorously for 5 min. Subsequently, 3200 μL of $NaBH_4$ (100 mM) were incorporated as a reducing agent. During this process, the solution's color transitioned from deep yellow to light yellow after 3 s, and eventually, to blue after stirring for 30 min at room temperature. The synthesized AgNPrs must be stored at 4 °C.

2.4. Optical identification of BAs

Optical identification of HIS and EDA by using AgNPrs as sensing probes was carried out at room temperature in the wavelength range of 200–800 nm. UV-vis spectra were recorded in quartz cuvette. The meat samples were measured equally and placed in microtubes. The prepared papers impregnated with AgNPrs were then utilized to detect the gases produced from both healthy and rotten meat samples. For the colorimetric recognition of HIS and EDA, the color change was monitored by mobile phone camera under a natural light source in solution and paper-based analytical device.

2.5. Construction of CATS

The design for the CATS was generated using CorelDRAW 5.6 software. The chips possess a substrate storage area that is linked to eight detection zones *via* eight channels. These chips were fabricated utilizing the method that we established in our earlier publication. To create the substrate for the CATS, the fiberglass papers were dipped in molten wax for 30 seconds and allowed to dry for 1 minute. The wax-free paper was then placed under the wax paper on top of a strong magnet. An iron pattern with eight prongs was heated to 150 °C for 5 min and used as a stamp on the papers. The magnet and iron pattern interaction created hydrophilic channels and hydrophobic areas on the wax-free paper (Scheme 1).

3. Results and discussion

3.1. Characterization and stability of sensing probe (Ag NPrs)

Nanoparticle characterization and stability was done according to our previous work.[30–32] Briefly, several techniques, including UV-vis spectroscopy, DLS, zeta potential, SEM, TEM, and AFM, were used to characterize the suggested sensing probes. One of the simplest ways to recognize metal nanoparticles and one that is frequently used to determine their size and shape is UV-vis. The produced Ag NPrs are blue and exhibit UV-vis absorption at wavelengths of 337, 477, and 705 nm. Ag NPrs's out-of-plane and in-plane quadrupole resonances are represented by the first two absorption bands, which have wavelengths of 337 and 477 nm, respectively. The Ag NPrs in-plane dipole resonance is another cause of the 705 nm band.[33,34] Zeta potential
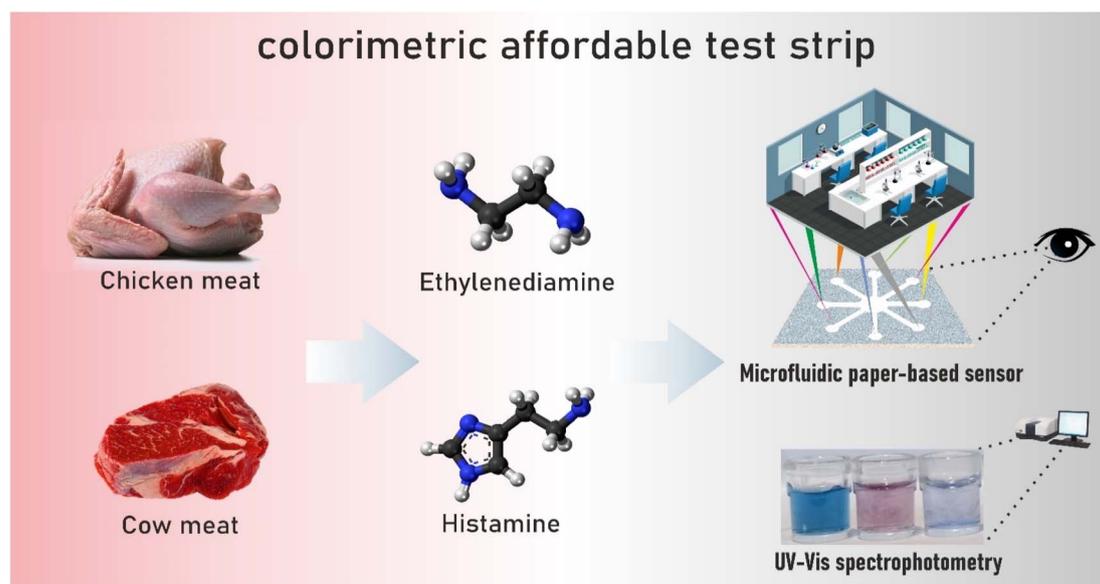
Scheme 1 Illustrated synthesis of AgNPrs, preparing of CATS, stabilization procedure, and interaction of optical probe with analyte.

© 2024 The Author(s). Published by the Royal Society of Chemistry

measurement is a practical method for determining the stability and surface charge of nanoparticles. With rising zeta potential, particle size increases and aggregation reduce. Nanoparticles with zeta potential larger than −30 and +30 mV show high stability.[35] The produced nanoparticles' zeta potential was −67.5 mV, indicating that they are stable enough. Using DLS, particle distribution profiles were assessed. The produced nanoparticles have a radius of 0.84 nm (Fig. S1 (see ESI)†). Direct imaging of atomic structures and crystallographic specimens was done using TEM imaging. The triangle-shaped structure is visible in the captured photos.

3.2. Optical discrimination of HIS and EDA

In solutions made from sensing probes, optical exams were carried out utilizing UV-vis spectroscopy method. The ability of the newly developed probes to detect HIS and EDA was first assessed. Then, it was investigated how sensitive and selective the sensing probes were in both the reference and actual samples.

3.3. Analysis of sensing probes' detection behavior

Nanomaterials can be recognized by a variety of physical and chemical characteristics. These characteristics are related to the surface-to-volume ratio.[36] As the particle size reduces and the surface area grows, the surface-to-volume ratio rises.[37] As a result, surface atoms and molecules are crucial to nanoparticles and influence their characteristics. Among the chemical and physical traits, optical capabilities are very significant and are frequently used in rapid and simple assessment techniques.[38] Many phenomena, including transmission, absorption, reflection, light scattering, transmission, and fluorescence, are produced when light interacts with nano systems.[39] For instance, Ag NPs are recognized by bands of intense absorption, but changes in the environment or exposure to analytes cause the bond characteristics to alter.[40] In the field of optical chemosensing of certain analytes, this sensitivity to the environment can be employed. A surface plasmon phenomenon happens when the light beam interacts with the solution, indicating the existence of nanoparticles and manifesting as a strong peak in the visible spectrum.[41] A particular phenomenon in metal nanoparticles, particularly AgNPs, is known as local surface plasmon resonance, and it is dependent on the dielectric constant of its surroundings.[37] Ag NPs generate a light effect known as the surface plasmon absorption band because of their free electrons. This effect is brought about by the combined vibration of the electron nanoparticles in the light wave resonance at the aqueous suspension.[39] The plasmon absorption shifts towards a lower energy wavelength and red as the size of the nanoparticles increases. Moreover, the absorption peak widens, indicating the development of the suspension and the aggregation. A steady dielectric shift caused by the presence of the analyte can be seen as a change in hue and a change in the location and amount of absorption.[42] Thus, before and after interaction with the proposed analytes, UV-vis spectroscopy of the sensing probe was recorded (with a volume ratio of 1 : 1).

The produced Ag NPrs are blue in color and exhibit UV-vis absorption at wavelengths of 337, 477, and 705 nm, as can be shown in Fig. 1. According to,[33,34] the first two absorption bands (337 and 477 nm) represent the out-of-plane and in-plane quadrupole resonances of Ag NPrs, respectively. The AgNPrs in-plane dipole resonance is also responsible for the 705 nm band. The form of the Ag NPrs has a significant impact on the color and in-plane bipolar resonance peak. By adding analytes, the dipole resonance peak in the plane has changed significantly. Thus, in the presence of HIS, it has increased significantly, and the peak related to quadrupolar excitation inside the plate has increased. In the presence of ethylene diamine, a shift in the peak corresponding to the in-plane dipole resonance was observed. These changes can be attributed to HIS etching on the prism silver tips. The changes can also be seen in the sample solutions, which allows the analysis of analytes in the solution. With the start of etching, the prisms change shape and turn into AgNPrs with a purple color. After one hour, the color of the solution changes to orange, which is probably due to the long-term exposure to the etching disc. Also, after one hour, no significant changes were observed in the absorption rate of the probe in the presence or absence of HIS, while in the presence of ethylene diamine, there were significant changes and the absorption rate decreased drastically. These comes about demonstrate that location of BAs with this triangular AgNPrs test is amazingly touchy to the nanoprism shape *versus* the top position of the in-plane dipole reverberation. The results show that a prominent change has been made in the surface, composition, and shape of nanoparticles, leading to a change in color and characteristic wavelength. Thus, a color change from blue to orange occurs along with an LSPR blue shift towards lower wavelengths.

3.4. Sensing mechanism of colorimetric detection of BAs by AgNPrs

As previously mentioned, the target BAs contain primary amines in different structure that can anchor onto the surface of the AgNPrs. This binding can be due to the direct interaction between nitrogen and Ag, and it can be considered as well in terms of an electrostatic interaction between the amine groups of BAs and NPs, which consequently induce the aggregation of AgNPs. So, AgNPrs offer an excellent platform for the colorimetric detection of BAs, which are organic compounds with biological functions that can be indicative of food freshness and safety. This sensing mechanism of BAs by AgNPrs is mainly attributed to the unique properties of AgNPrs, particularly their SPR effect. The colorimetric detection mechanism is based on the interaction between AgNPrs and BAs, which leads to a change in the color of the AgNP solution. Specifically, when BAs interact with AgNPs, they can cause aggregation of the nanoparticles, leading to a shift in the SPR and hence a color change. It is not clear if the interactions of the BAs to the plasmonic NPs are based on electrostatic interaction between amines and carboxylic acid or the chemical binding of amine to the Ag. The electrostatic interaction, including the protonated amino group of BAs and the negatively charged carboxylic acid
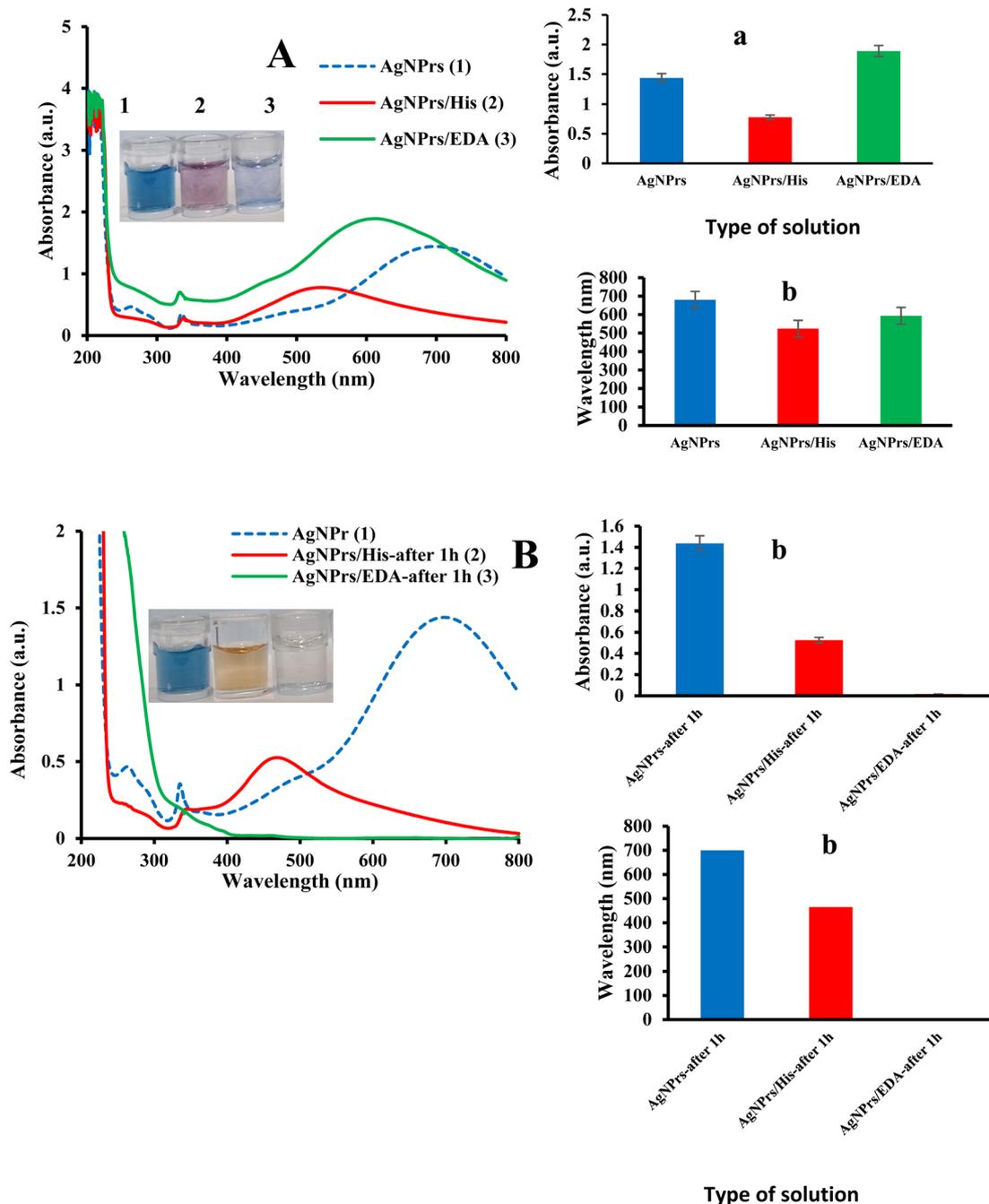
Fig. 1 The UV-vis spectra of sensing probes in the presence and absence of HIS and EDA immediately (A) and after 1 h (B). Inset: histogram of Abs (a.u.) (a) and wavelength (b) *versus* type of analyte. Concentrations of HIS&EDA were 10 μM.

on the NPs, should be pH dependent. According to their aggregation responses, we found that the aggregation behaviors of the AgNPs showed that the UV-vis spectra of the AgNPs did not change in the presence of HIS at the all pH regimes, which can confirm that these two BAs did not have an electrostatic interaction. This could be due to the presence of an aromatic ring in their structure, which probably provided a high spatial hindrance to bind to the AgNPs. On the other hand, the aggregation of the AgNPs in the presence of EDA with the aliphatic amine groups decreased by increasing the pH values,

which can also emphasize the strong interaction of the protonated BAs and the negative charge of the citrate group on the AgNPs.

3.5. Analytical evaluation for determination of His and EDA

According to the examination results of the ability of introduced sensing probes to monitor His and EDA, their ability at low concentrations of analyte was also evaluated. Therefore, UV-vis spectrophotometric measurements of separate reaction systems

determined the relationship between His and EDA concentration and adsorption. For this purpose, analyte solutions with different concentrations were prepared and mixed with a sensing probe in a volume ratio of 1 : 1 v : v. The absorption spectra recorded in the range of 250 to 800 nm are exhibited in Fig. S2 (see ESI).† In addition, the adsorption of chemosensor *versus* concentration ratio is also presented in Fig. S2 (see ESI).† Then, important analytical parameters such as linear range and low limit of quantification (LLOQ) were obtained from calibration curves. As can be seen, at the concentration of 0.01 and 0.005 M HIS, a colour change and a blue shift are seen. While at lower concentrations, no color change was observed, and a slight blue shift was observed. The results showed a linear relationship between concentrations 0.1 μM to 0.01 mM. The low limit of quantification was 0.1 μM. In EDA, a shift in absorption peak from 550 to 630 is observed with decreasing concentration. Colorimetric changes also show the probe's ability to detect EDA at low concentrations. The linear range for the detection of EDA was 0.05 to 1 μM with an LLOQ of 0.05 μM.

3.6. Selectivity of the analytical process in standard samples

Selectivity is one of the most significant factors for the analytical evaluation of chemosensors traits in a biosensor. In fact, specificity indicates the ability of a sensing probe to detect an analyte in a specimen containing other contaminants. Therefore, to evaluate the selectivity of the proposed probe for the recognition of analytes, their colorimetric and spectrophotometric behavior was done. For this purpose, we also evaluated the detection probe's ability to identify some amino acids. As seen in Fig. S3 (see ESI),† the diagnostic probe can specifically detect both analytes. In addition, the ability of the probe to detect analytes in the presence of potential interferers was also evaluated. The obtained results showed that there was a change in the amount of HIS absorption in the presence of the interventionists. Colorimetric studies also confirm the ability of the probe to detect HIS in the presence of interfering substances. In the case of EDA, the presence of intervenors has led to significant changes in the amount of absorption, which can be said that the presence of intervenors can affect its detection.

3.7. Detection of HIS and EDA in meat

Due to their high protein and amino acid content, meat and meat products are susceptible to developing BAs. Proteolytic activity might develop due to a protracted storage period or in production. The proteolysis of proteins into significant peptides, which are later degraded into oligopeptides and free amino acids, can increase the quantities of BAs during storage.[5] In addition to inherent effects like dryness, salt chloride action in some meat-derived products, and increased acidity, proteolysis is also stimulated by microbial activity during fermentation and other food manufacturing processes. While it has been reported that BAs accumulate in fermented meat products, meat fermentation helps to preserve against different pathogenic and spoilage bacteria. BAs, whether individually or combined, can serve as important indicators of freshness, quality, and spoilage in meat and meat products due to their

significant impact on health and their distinct implications for food hygiene.[43] Therefore, the ability of the probe to detect analytes in spiked samples of fresh and spoiled meat was evaluated. Evaluation was performed in the liquid and vapor phases.

3.7.1. Optimization of analytes-probe ratio in liquid phase. The probe was mixed with control samples (resulting from centrifugation of meat samples without analytes) and analytes in different ratios. As seen in Fig. S4 (see ESI),† the colorimetric changes in the presence of EDA seem to be more significant with time. Therefore, it can be concluded that the reaction becomes more complete with the passage of time. The maximum amount of absorption was obtained in a 3 : 1 V : V ratio of probe and analyte. Therefore, the next investigations will be done with this ratio. Colorimetric studies show wavelength shift in HIS detection. Over time, the probe loses the ability to detect HIS in the meat sample.

3.7.2. Analysis of sensing probes' detection behavior. The performance of the probe was evaluated in the colorimetric detection of amine BAs in fresh and spoiled meat samples in the liquid phase. As seen in Fig. 2A, in the fresh meat sample, the absorption wavelength was higher than in the spiked meat sample with HIS and EDA. absorption wavelength in rotten meat samples was lower than in fresh meat, while the amount of BAs increased due to meat spoilage. Therefore, it can be said that in the meat sample, the absorption wavelength decreases with the increase in the target amount. The color changes show that the introduced probe is capable of detecting targets in the meat sample as well. After one hour, a change in absorption wavelength and colorimetric changes were observed (Fig. 2B).

3.7.3. Optical analysis in fresh and spoiled beef samples. In optimal conditions, a colorimetric probe was used to detect the amount of ethylene diamine and HIS in fresh and spoiled meat samples. As can be seen in Fig. 3 and S5 (see ESI),† the probe changes its color and absorption in the presence of EDA and HIS. This shows that the proposed probe can be used to detect target BAs in this column. Examining different concentrations of the target analytes showed a good linear relationship and the lowest limit of quantification (LLOQ). The results obtained from this work along with the results obtained from other reports presented in the detection of HIS are presented in Table 1.

In summary, we developed an optical and colorimetric biosensor for HIS and EDA detection, as Table 1 illustrates. The development of BAs's detecting platform based on optical sensing techniques has significant potential for the food safety. One of the advantages of this work is that, to the best of our knowledge, no report has been published on the detection of HIS and EDA based on the sensing probes introduced in this study. The proposed probes' suitability for HIS and EDA analysis was assessed through the application of UV-vis spectroscopy. The performance of the sensor presented in this study is compared to previous research, showing its improved sensitivity and linear detection range. Additionally, colorimetric studies were carried out using paper-based microfluidics, indicating the potential usefulness of these microfluidics in developing diagnostic kits for BAs. On the other hand, the off-
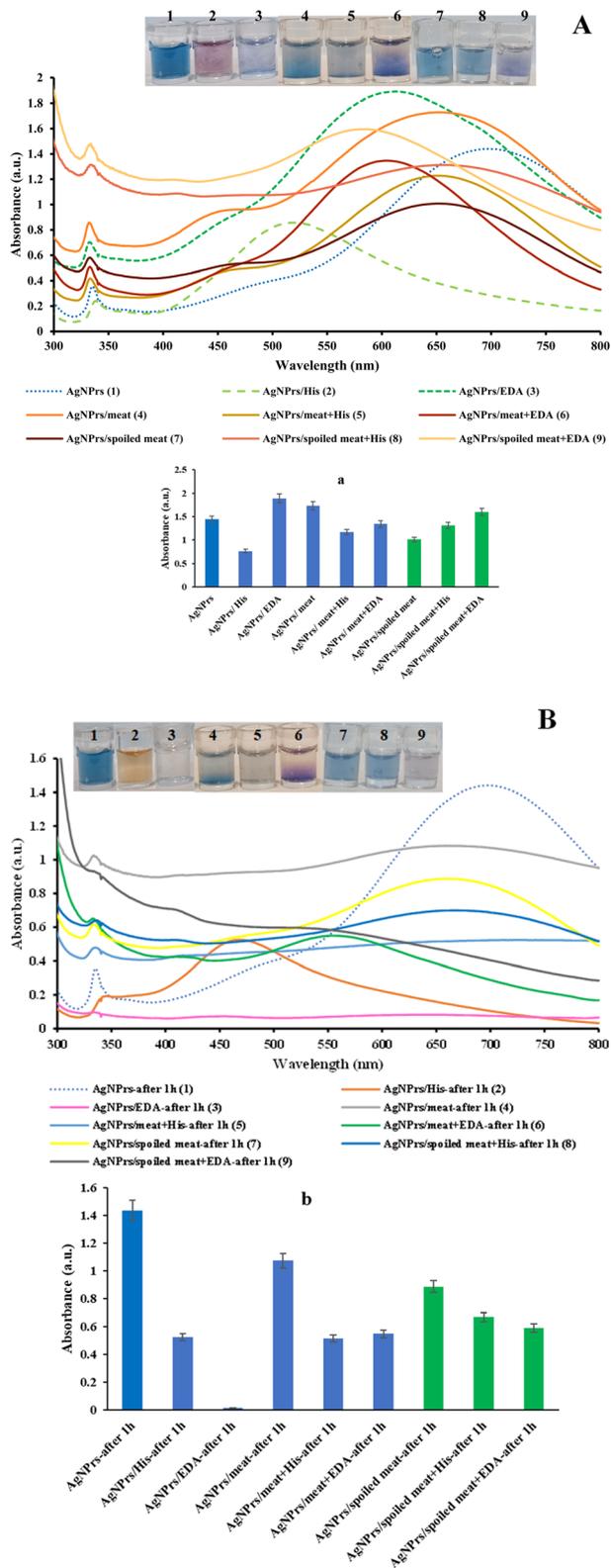
Fig. 2 The UV-vis spectra of sensing probes in the presence and absence of His and EDA at the fresh and rotten meat in different incubation time of 0 min (A) and 60 min (B). [a&b] Histogram of peak absorption *versus* incubation time of analyte.

the-shelf system is highly easy to use, sensitive, affordable, cost-effective, selective, and requires minimal time. It is also portable and compact. Substantial progress is still required in future research to integrate current biosensor technologies into standard clinical practice. The strengths of different biosensor systems should be integrated with electrochemical and optical transmission mechanisms to establish a universal sensing approach. Development of clinical protocols for sample management is considered crucial for comprehensive sample analysis. The lack of integrated detection systems indicates the need for further advancements. Thus, additional research and development in the field of science and technology are necessary to explore the integration of sensors, recognition elements, and transducers into a portable biosensor product relevant for all systems. Moreover, significant progress is lacking in *in vivo* multichannel biosensor techniques. Once engineering challenges, such as improving biocompatible materials and *in vivo* multi-signaling, are addressed, next-generation sensing and biosensing platforms could be widely employed for point-of-care screening and detection systems. In summary, this optical system is an innovative approach for in-depth analytical research.

3.7.4. Selectivity of AgNPrs probe for *in situ* analysis of BAs. One of the most important aspects of the analytical assessment of chemosensors is selectivity. A sensing probe's specificity is defined as its capacity to identify an analyte in a specimen that also contains other impurities. Consequently, a colorimetric and spectrophotometric analysis of the suggested probes' behavior was conducted to assess their selectivity for the identification of HIS and EDA. For this purpose, the nanoprism colorimetric probe, color changes and changes in absorbance in the presence of target analytes and interferents (glysin (Gly), tyrosine (Tyr), arginine (Arg), methionine (Met), dopamine (Dop), cysteine (Cys)) were evaluated in fresh and spoiled meat samples. As can be seen in Fig. S6A (see ESI),† in the presence of methionine and dopamine in the fresh meat sample, the absorption rate is higher than other interventions. If the color changes in the solution phase are seen only in the presence of methionine and cysteine. In Fig. S6B (see ESI),† the effect of interventionists has been investigated in the presence of target analytes. As can be seen, in the presence of tyrosine and cysteine, a color change is visible, which shows that these two items do not interfere with the colorimetric detection of HIS. According to the color changes created in the presence of ethylene diamine, it can be concluded that glycine, tyrosine, and arginine do not interfere in the detection of EDA (Fig. S7C (see ESI)†).

In the spoiled meat sample, colorimetric changes can be seen in the presence of glycine and cysteine, which shows that the introduced probe can detect them as well. Examining the effect of the intervention in the presence of HIS, which is presented in Fig. S8 (see ESI),† shows that the color change is seen only in the presence of cysteine. Therefore, it can be said that cysteine, cannot interfere in the detection of HIS in the trace of rotten meat. However, the examination of the absorption rate shows that the rejection of the presence of cysteine significantly changed the absorption rate. Regarding the detection of EDA,
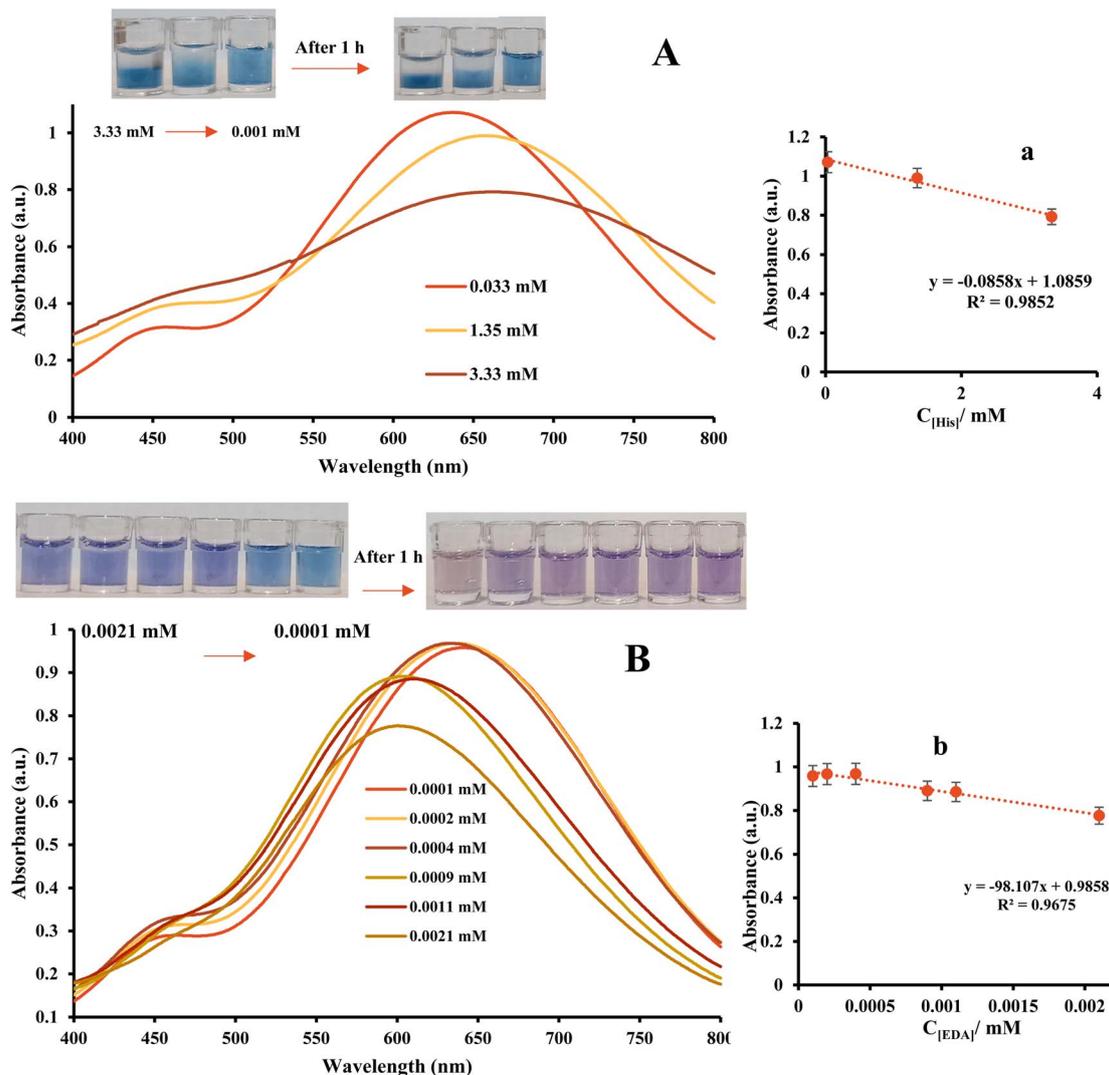
Fig. 3 The UV-vis spectra of AgNPrs in the presence of different concentration of (A) HIS (B) EDA at the fresh meat. [a&b] Calibration curve of HIS and EDA using optical chemosensor.

Table 1 Performance comparison of sensors for His and EDA detection with other previous reported sensors

Methods	Samples		Linear range (μM)	LOD/LLOQ (μM)	Ref.
Electrochemical	Spiked beer and wine samples		1–107	0.6	44
	Salted anchovies		16–101	17.2	45
	Human serum and fish tuna		$(0.35–35) \times 10^{-3}$	0.11×10^{-3}	46
	Human serum and canned tuna fish		$(0.078–250) \times 10^{-3}$	0.026×10^{-3}	47
	Canned fish		45–900	5.58	48
	Beer and wine		4.5–720	1.26	49
	Octopus		—	8.1	50
	Cheese		0.38–11	0.38	51
	Spiked tuna and mackerel extracts		45–675	8.7	52
Colorimetry	Fresh meat	HIS	1–3330	1	This work
		EDA	0.1–2.1	0.1	
	Spoiled meat	HIS	3.3–2330	3.3	
		EDA	0.1–3.3	0.1	

the results of the colorimetric and absorption studies show that the intervenors did not have a significant effect on the detection.

3.8. Development of a CATS for colorimetric detection of His and EDA

In addition to the promising outcomes obtained using UV-vis spectrophotometry, recent studies have shown considerable interest in paper-based sensors due to their user-friendly nature and affordability, resulting in significant advancements. These sensors have great potential for low-cost detection of various analytes and are expected to be used for rapid analysis of different targets in the future.[31] Tools that are quick, focused, exclusive, and reasonably priced are particularly useful for on-site environmental inspections. Papers have been thought of as a viable substrate for the construction of such devices because to their benefits such as low cost, commercial availability, and simple design. Moreover, papers may flow fluids into their channels without the aid of a pump or other external force because they are constructed of ecologically benign cellulose fibers and have capillary qualities. In this study, different concentrations of HIS and EDA were evaluated on CATS modified AgNPrs in standard and meat samples. The obtained results show that the prepared paper-based substrates can detect analytes in both standard and meat samples.

The provided data discusses the development and evaluation of a CATS for the colorimetric detection of His and EDA in standard and meat samples. In this study AgNPrs utilized as the novel sensing element/probe which stabilized on CATS to generate the new generation of nanomaterials in order to create and develop the paper-based biosensors for food industry which assure the high quality of products health. BAs, produced by microorganisms through the decarboxylation of amino acids, can have adverse health effects if consumed in high concentrations. The paper-based CATS decorated with AgNPrs suggests a simple, environmentally friendly, and cost-effective approach for on-site diagnostic purposes.

The obtained experimental results are presented in Fig. 4, 5 and S9 (see ESI)† regarding paper-based AgNPrs substrate for colorimetric detection of His and EDA. Fig. 4 demonstrates the results of CATS modified by AgNPrs for the detection of different concentration of His in the eight-zone corresponding to the concentrations of 0.001, 0.0033, 0.01, 0.033, 0.35, 1.35, 2.33, and 3.33 mM, respectively and EDA in the eight-zone corresponding to the concentrations of 0.0001, 0.0002, 0.0004, 0.0009, 0.0015, 0.0021, 0.0025, and 0.0033 mM in standard samples. The results demonstrate the visual detection of His and EDA through color changes in different zones of the paper-based device, corresponding to specific analyte concentrations. This indicates that the CATS can successfully identify the target analytes (BAs) in both standard and meat samples.

Fig. 5 depicts the specificity analysis of the chemosensing performance of optical probes for individual identification of some interference using CATS in standard samples. The results show that the AgNPrs-based sensor exhibits specificity towards HIS and EDA, as evidenced by the absence of significant interference from other tested compounds.

In Fig. S8,† CATS modified by AgNPrs applied for the detection of different concentrations of His and EDA in meat samples. Similar to Fig. 4, the images demonstrate the colorimetric detection of His and EDA in different zones of the paper-based device, indicating the potential applicability of the biosensor in real food samples. The development of a CATS decorated AgNPrs for the colorimetric detection of His and EDA in standard and meat samples shows promising results. The utilization of paper as a substrate offers several advantages, including low cost, commercial availability, and simple design. Additionally, the capillary qualities of paper enable the flow of fluids without the need for external forces, making it suitable for on-site environmental inspections. The presented results indicate that the paper-based biosensor can effectively detect His and EDA in both standard and meat samples. The color changes observed in the paper-based interface correspond to different concentrations of the target analyte, providing a visual and qualitative detection method. This demonstrates the
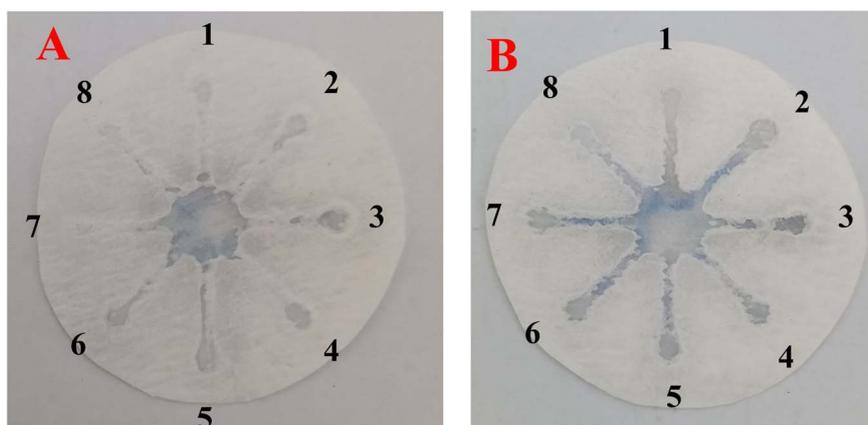

Fig. 4 Photographic images of CATS modified by AgNPrs for detection of different concentration of (A) His (zones 1 to 8 corresponding to the concentrations of 0.001, 0.0033, 0.01, 0.033, 0.35, 1.35, 2.33, and 3.33 mM, respectively) and (B) EDA (zones 1 to 8 corresponding to the concentrations of 0.0001, 0.0002, 0.0004, 0.0009, 0.0015, 0.0021, 0.0025, and 0.0033 mM, respectively) in standard samples.
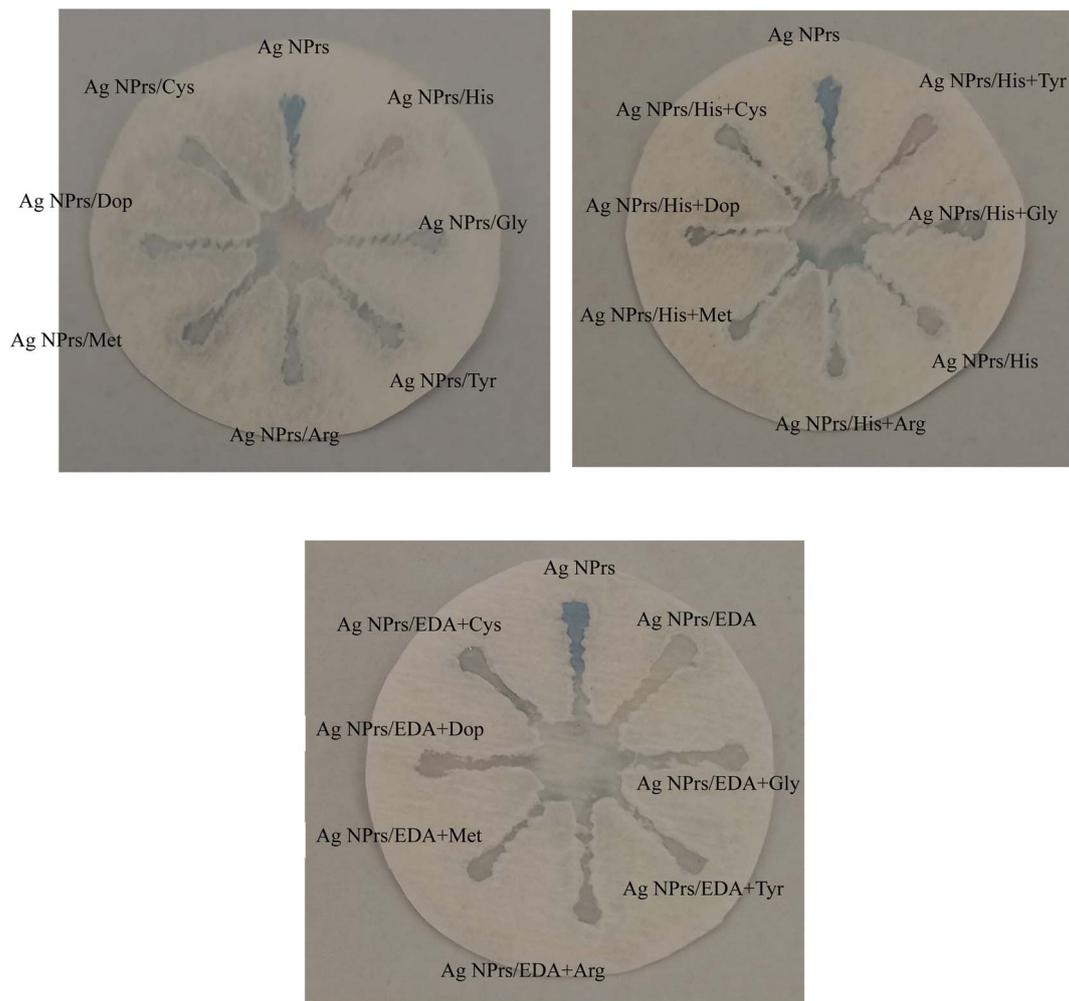
Fig. 5 Specificity analysis of chemosensing performance of optical probes for individual identification of some interference using CATS in standard samples.

potential of the biosensor as a rapid and cost-effective tool for the detection of BAs in food samples.

The specificity analysis depicted in Fig. 5 confirms the selectivity of the AgNPrs-based sensor towards His and EDA. The absence of significant interference from other compounds tested in standard samples suggests that the biosensor can accurately distinguish the target analytes from potential interfering substances, enhancing its reliability and applicability in practical food analysis. Furthermore, the successful detection of His and EDA in meat samples, as shown in Fig. S8,† highlights the potential of the paper-based biosensor for real food applications. The ability to detect these BAs in meat samples is crucial for ensuring food safety and preventing the harmful effects associated with their consumption.

Overall, the development of a CATS using AgNPrs as a sensing element presents a promising approach for the sensitive and selective detection of His and EDA in food samples. The simplicity, affordability, and potential for on-site diagnostics make this biosensor an attractive tool for food quality analysis and control, contributing to the overall goal of ensuring food safety and preventing adverse health effects. Further research and validation studies are warranted to assess the biosensor's performance in a broader range of food matrices and to explore its potential for large-scale implementation. In the paper-based biosensor for the colorimetric detection of His and EDA, the mechanism involves the use of AgNPrs as the sensing element. The AgNPrs undergo a specific chemical reaction with His and EDA, leading to a visible color change that can be observed with the naked eye.

3.9. Gas phase studies of BAs in meat samples

According to the results obtained in the solution and CATS, in order to complete the study, investigations were also carried out in the gas phase. For this purpose, 5 μL of optical probe (AgNPrs) were placed on paper and exposed to HIS vapor, ethylene diamine, fresh meat and rotten meat. An empty container was also considered as control (Video 1†). The results obtained, which can be seen in the video files (see ESI†), show that the probe can detect BAs in the gas from rotten meat. In addition, we checked for rotten meat at weekly intervals (Videos

2 to 5†). The results showed that with the passage of time, the gas produced increased, and a tangible color change was seen. The obtained results can give a new approach in the food industry in order to check the quality of meat with easy and cheap methods and in the place of development.

In conclusion, wax screen printing is a simple and inexpensive way to make CATS. As previously mentioned, wax is a cheap material and can be obtained from anywhere; it is also environmentally friendly. This method requires a wax printer and inexpensive printing plates. Also, the wax printing method is done without the use of a sterile room, ultraviolet lamp, organic solvents or complicated equipment. Another important advantage of this method compared to previous methods is that it only requires a common hot plate or similar surface and a common printing plate that can be produced anywhere in the world, making this method a great way to make CATS in developing countries.

Also, the clinical utilization of colorimetric sensing of BAs holds great promise for various diagnostic and monitoring purposes. It can be employed for the early detection of certain diseases (like allergic reaction), monitoring of treatment efficacy, and assessment of disease progression. Additionally, colorimetric sensing can facilitate the development of personalized medicine approaches by enabling the monitoring of individual variations in BAs levels. So, the clinical utilization of colorimetric sensing of BAs represents a valuable tool in modern healthcare practice. Further research and development in this field are warranted to fully harness the potential of colorimetric sensing for the diagnosis and management of BAs-related disorders. Also, future BAs detection may find chemo-sensor technologies appealing because of their quick readout times, affordability, sensitivity, selectivity, and portability.

4. Conclusion

In summary, this study suggested and validated an innovative colorimetric/spectrophotometric method, for rapid discrimination of two BAs in real samples using AgNPrs as optical probe. Also, the CATS used in this work demonstrated excellent stability and reproducibility in real-time colorimetric identification and accurate determination of BAs in the presence of interfering species. In addition, the response time of the system was rapid, achieving 90% of the response within 2 minutes, and the distinct color differences allowed easy identification of the amines even by visual observation alone. The system presented a fast visual method for HIS and EDA analysis in the range of 0.1 μM to 0.01 mM, with an LLOQ of 0.1 μM and 0.05 to 1 μM, with an LLOQ of 0.05 μM, respectively by measuring the UV-vis absorption wavelength. Obtained results show that, future studies should consider controlling or eliminating these interfering agents. The prepared assay showed only one limitation that it could not be reused for strong reactions. We are dedicating our efforts to overcoming this limitation and enhancing CATS' capability for the early detection of meat spoilage. Nevertheless, a long-term stability would allow the CATS to be used as a promising tool for monitoring different BAs involved in food safety and disease diagnosis. The system's excellent

features suggest that these devices could be commercialized in the near future, replacing complex laboratory methods.

Conflicts of interest

There are no conflicts to declare.

Acknowledgements

References

1 A. Marcobal, M. Polo, P. Martın-Alvarez and M. Moreno-Arribas, Biogenic amine content of red Spanish wines: comparison of a direct ELISA and an HPLC method for the determination of histamine in wines, *Food Res. Int.*, 2005, **38**(4), 387–394.

2 L. He, Z. Xu, T. Hirokawa and L. Shen, Simultaneous determination of aliphatic, aromatic and heterocyclic biogenic amines without derivatization by capillary electrophoresis and application in beer analysis, *J. Chromatogr. A*, 2017, **1482**, 109–114.

3 Y. Özogul and F. Özogul, *Biogenic Amines Formation, Toxicity, Regulations in Food. Biogenic Amines in Food: Analysis, Occurrence and Toxicity*, 2019, pp. 1–17.

4 W. Wójcik, M. Łukasiewicz and K. Puppel, Biogenic amines: formation, action and toxicity–a review, *J. Sci. Food Agric.*, 2021, **101**(7), 2634–2640.

5 A. Durak-Dados, M. Michalski and J. Osek, Histamine and other biogenic amines in food, *J. Vet. Res.*, 2020, **64**(2), 281–288.

6 B. ten Brink, C. Damink, H. Joosten and J. H. In't Veld, Occurrence and formation of biologically active amines in foods, *Int. J. Food Microbiol.*, 1990, **11**(1), 73–84.

7 P. Visciano, M. Schirone and A. Paparella, An overview of histamine and other biogenic amines in fish and fish products, *Foods*, 2020, **9**(12), 1795.

8 S. Rossi, C. Lee, P. Ellis and L. Pivarnik, Biogenic amines formation in bigeye tuna steaks and whole skipjack tuna, *J. Food Sci.*, 2002, **67**(6), 2056–2060.

9 T.-t Zhou, A. Yigaimu, T. Muhammad, P.-l Jian, L.-n Sha and S.-b Zhang, Novel carrier-mediated membrane-assisted three-phase liquid–liquid extraction coupled with liquid chromatography–mass spectrometry for the determination of eight biogenic amines in foods, *Food Chem.*, 2022, **387**, 132857.

10 A. Önal, S. E. K. Tekkeli and C. Önal, A review of the liquid chromatographic methods for the determination of biogenic amines in foods, *Food Chem.*, 2013, **138**(1), 509–515.

11 M. Papageorgiou, D. Lambropoulou, C. Morrison, J. Namieśnik and J. Płotka-Wasylka, Direct solid phase microextraction combined with gas chromatography–Mass

spectrometry for the determination of biogenic amines in wine, *Talanta*, 2018, **183**, 276–282.

12 Á. Kovács, L. Simon-Sarkadi and K. Ganzler, Determination of biogenic amines by capillary electrophoresis, *J. Chromatogr. A*, 1999, **836**(2), 305–313.

13 G. Sagratini, M. Fernández-Franzón, F. De Berardinis, G. Font, S. Vittori and J. Mañes, Simultaneous determination of eight underivatised biogenic amines in fish by solid phase extraction and liquid chromatography–tandem mass spectrometry, *Food Chem.*, 2012, **132**(1), 537–543.

14 H. Vasconcelos, L. C. Coelho, A. Matias, C. Saraiva, P. A. Jorge and J. M. de Almeida, Biosensors for biogenic amines: A review, *Biosensors*, 2021, **11**(3), 82.

15 A. Önal, A review: Current analytical methods for the determination of biogenic amines in foods, *Food Chem.*, 2007, **103**(4), 1475–1486.

16 A. A. Lahcen, S. Rauf, T. Beduk, C. Durmus, A. Aljedaibi, S. Timur, *et al.*, Electrochemical sensors and biosensors using laser-derived graphene: A comprehensive review, *Biosens. Bioelectron.*, 2020, **168**, 112565.

17 I. I. Ebralidze, N. O. Laschuk, J. Poisson and O. V. Zenkina, *Colorimetric Sensors and Sensor Arrays. Nanomaterials Design for Sensing Applications*, Elsevier, 2019, pp. 1–39.

18 X. Zhong, D. Huo, H. Fa, X. Luo, Y. Wang, Y. Zhao, *et al.*, Rapid and ultrasensitive detection of biogenic amines with colorimetric sensor array, *Sens. Actuators, B*, 2018, **274**, 464–471.

19 Y. Wang, Y. Sun, H. Dai, P. Ni, S. Jiang, W. Lu, *et al.*, A colorimetric biosensor using Fe3O4 nanoparticles for highly sensitive and selective detection of tetracyclines, *Sens. Actuators, B*, 2016, **236**, 621–626.

20 A. I. Danchuk, N. S. Komova, S. N. Mobarez, S. Y. Doronin, N. A. Burmistrova, A. V. Markin, *et al.*, Optical sensors for determination of biogenic amines in food, *Anal. Bioanal. Chem.*, 2020, **412**, 4023–4036.

21 K. Kant, M.-A. Shahbazi, V. P. Dave, T. A. Ngo, V. A. Chidambara, L. Q. Than, *et al.*, Microfluidic devices for sample preparation and rapid detection of foodborne pathogens, *Biotechnol. Adv.*, 2018, **36**(4), 1003–10024.

22 S. A. Papatheodorou, T. Tsironi, M. Giannakourou, P. Halvatsiotis and D. Houhoula, Application of microfluidic paper-based analytical devices (μPADs) for food microbial detection, *J. Sci. Food Agric.*, 2022, **103**(4), 2215.

23 B. P. Correia, M. P. Sousa, C. E. A. Sousa, D. Mateus, A. I. Sebastião, M. T. Cruz, A. M. Matos, A. C. Pereira and F. T. C. Moreira, *Cellulose*, 2022, **29**, 9311–9322.

24 I. Papautsky, L. Shen and R. Naik, Method and System for Analyzing a Colorimetric Assay, WO2013116831A1, 2013.

25 A. T. Hoang, Y. B. Cho and Y. S. Kim, *Sens. Actuators, B*, 2017, **251**, 1089–1095.

26 L. Minhua, S. Vince, R. A. Budd and E. G. Colgan, Accurate Colorimetric Based Test Strip Reader System, *US Pat.* US11307147B2, 2018.

27 V. Amendola, O. M. Bakr and F. Stellacci, A study of the surface plasmon resonance of silver nanoparticles by the discrete dipole approximation method: effect of shape, size, structure, and assembly, *Plasmonics*, 2010, **5**, 85–97.

28 K. Nitinaivinij, T. Parnklang, C. Thammacharoen, S. Ekgasit and K. Wongravee, Colorimetric determination of hydrogen peroxide by morphological decomposition of silver nanoprisms coupled with chromaticity analysis, *Anal. Methods*, 2014, **6**(24), 9816–9824.

29 J. Haber and K. Sokolov, Synthesis of stable citrate-capped silver nanoprisms, *Langmuir*, 2017, **33**(40), 10525–10530.

30 A. Saadati, F. Farshchi, M. Hasanzadeh, Y. Liu and F. Seidi, Colorimetric and naked-eye detection of arsenic (III) using a paper-based colorimetric device decorated with silver nanoparticles, *RSC Adv.*, 2022, **12**(34), 21836–21850.

31 F. Farshchi, A. Saadati, M. Hasanzadeh, Y. Liu and F. Seidi, Optimization of a silver-nanoprism conjugated with 3, 3′, 5, 5′-tetramethylbenzidine towards easy-to-make colorimetric analysis of acetaldehyde: a new platform towards rapid analysis of carcinogenic agents and environmental technology, *RSC Adv.*, 2023, **13**(9), 6225–6238.

32 A. Saadati, F. Farshchi, M. Hasanzadeh and F. Seidi, A microfluidic paper-based colorimetric device for the visual detection of uric acid in human urine samples, *Anal. Methods*, 2021, **13**(35), 3909–3921.

33 G. S. Métraux and C. A. Mirkin, Rapid thermal synthesis of silver nanoprisms with chemically tailorable thickness, *Adv. Mater.*, 2005, **17**(4), 412–415.

34 J. E. Millstone, S. J. Hurst, G. S. Métraux, J. I. Cutler and C. A. Mirkin, Colloidal gold and silver triangular nanoprisms, *Small*, 2009, **5**(6), 646–664.

35 P. Abdollahiyan, M. Hasanzadeh, P. Pashazadeh-Panahi and F. Seidi, Application of Cys A@ AuNPs supported amino acids towards rapid and selective identification of Hg (II) and Cu (II) ions in aqueous solution: An innovative microfluidic paper-based (μPADs) colorimetric sensing platform, *J. Mol. Liq.*, 2021, **338**, 117020.

36 D. Vilela, M. C. González and A. Escarpa, Sensing colorimetric approaches based on gold and silver nanoparticles aggregation: Chemical creativity behind the assay, *Anal. Chim. Acta*, 2012, **751**, 24–43.

37 K. M. Mayer and J. H. Hafner, Localized surface plasmon resonance sensors, *Chem. Rev.*, 2011, **111**(6), 3828–3857.

38 S. Szunerits and R. Boukherroub, Sensing using localised surface plasmon resonance sensors, *Chem. Commun.*, 2012, **48**(72), 8999–9010.

39 P. Prosposito, L. Burratti and I. Venditti, Silver nanoparticles as colorimetric sensors for water pollutants, *Chemosensors*, 2020, **8**(2), 26.

40 K. Shiva Prasad, G. Shruthi and C. Shivamallu, Functionalized silver nano-sensor for colorimetric detection of Hg2+ ions: facile synthesis and docking studies, *Sensors*, 2018, **18**(8), 2698.

41 K. A. Willets and R. P. Van Duyne, Localized surface plasmon resonance spectroscopy and sensing, *Annu. Rev. Phys. Chem.*, 2007, **58**, 267–297.

42 V. N. Mehta, A. K. Mungara and S. K. Kailasa, Dopamine dithiocarbamate functionalized silver nanoparticles as

colorimetric sensors for the detection of cobalt ion, *Anal. Methods*, 2013, **5**(7), 1818–1822.

43 M. Schirone, L. Esposito, F. D'Onofrio, P. Visciano, M. Martuscelli, D. Mastrocola, *et al.*, Biogenic amines in meat and meat products: a review of the science and future perspectives, *Foods*, 2022, **11**(6), 788.

44 S. Li, T. Zhong, Q. Long, C. Huang, L. Chen, D. Lu, *et al.*, A gold nanoparticles-based molecularly imprinted electrochemical sensor for histamine specific-recognition and determination, *Microchem. J.*, 2021, **171**, 106844.

45 W. Henao-Escobar, O. Domínguez-Renedo, M. A. Alonso-Lomillo and M. J. Arcos-Martínez, A screen-printed disposable biosensor for selective determination of putrescine, *Microchim. Acta*, 2013, **180**, 687–693.

46 A. M. Mahmoud, S. A. Alkahtani, B. A. Alyami and M. M. El-Wekil, Dual-recognition molecularly imprinted aptasensor based on gold nanoparticles decorated carboxylated carbon nanotubes for highly selective and sensitive determination of histamine in different matrices, *Anal. Chim. Acta*, 2020, **1133**, 58–65.

47 M. H. Mahnashi, A. M. Mahmoud, K. Alhazzani, A. Alanazi, M. M. Algahtani, A. M. Alaseem, *et al.*, Enhanced molecular imprinted electrochemical sensing of histamine based on signal reporting nanohybrid, *Microchem. J.*, 2021, **168**, 106439.

48 P. Nakthong, T. Kondo, O. Chailapakul and W. Siangproh, Development of an unmodified screen-printed graphene electrode for nonenzymatic histamine detection, *Anal. Methods*, 2020, **12**(44), 5407–5414.

49 Z. S. Stojanović, E. Mehmeti, K. Kalcher, V. Guzsvány and D. M. Stanković, SWCNT-modified carbon paste electrode as an electrochemical sensor for histamine determination in alcoholic beverages, *Food Anal. Methods*, 2016, **9**, 2701–2710.

50 W. Henao-Escobar, L. Del Torno-de Román, O. Domínguez-Renedo, M. Alonso-Lomillo and M. Arcos-Martínez, Dual enzymatic biosensor for simultaneous amperometric determination of histamine and putrescine, *Food Chem.*, 2016, **190**, 818–823.

51 B. Dalkıran, C. Kaçar, E. Can, P. E. Erden and E. Kılıç, Disposable biosensors based on platinum nanoparticle-modified screen-printed carbon electrodes for the determination of biogenic amines, *Monatsh. Chem.*, 2020, **151**, 1773–1783.

52 R. Torre, E. Costa-Rama, H. P. Nouws and C. Delerue-Matos, Diamine oxidase-modified screen-printed electrode for the redox-mediated determination of histamine, *J. Anal. Sci. Technol.*, 2020, **11**, 1–8.